Materials Science & Engineering C 99 (2019) 1191–1198

Contents lists available at ScienceDirect

Materials Science & Engineering C

journal homepage: www.elsevier.com/locate/msec

Injectable, thermosensitive, fast gelation, bioeliminable, and oxygen sensitive hydrogels

Chao Li[a,1], Zheng Huang[a,1], Ning Gao[a,b,1], Jie Zheng[c], Jianjun Guan[a,b,*]

[a] Department of Materials Science and Engineering, The Ohio State University, Columbus, OH 43210, USA
[b] Department of Mechanical Engineering and Materials Science, Washington University in St. Louis, St. Louis, MO 63130, USA
[c] Mallinckrodt Institute of Radiology, Washington University in St. Louis, St. Louis, MO 63110, USA

ARTICLE INFO

Keywords:
Bioeliminable hydrogel
Thermosensitive hydrogel
Oxygen sensitive hydrogel
Tetrathiatriarylmethyl radicals

ABSTRACT

The decrease of tissue oxygen content due to pathological conditions leads to severe cell death and tissue damage. Restoration of tissue oxygen content is the primary treatment goal. To accurately and efficiently assess efficacy of a treatment, minimally invasive, and long-term detection of oxygen concentration in the same tissue location represents a clinically attractive strategy. Among the different oxygen concentration measurement approaches, electron paramagnetic resonance (EPR) has the potential to accomplish this. Yet there lacks injectable EPR probes that can maintain a consistent concentration at the same tissue location during treatment period to acquire a stable EPR signal, and can finally be eliminated from body without retrieval. Herein, we developed injectable and bioeliminable hydrogel-based polymeric EPR probes that exhibited fast gelation rate, slow weight loss rate, and high oxygen sensitivity. The probe was based on N-Isopropylacrylamide (NIPAAm), 2-hydroxyethyl methacrylate (HEMA), dimethyl-γ-butyrolactone acrylate (DBA), and tetrathiatriarylmethyl (TAM) radical. The injectable probes can be implanted into tissues using a minimally invasive injection approach. The high gelation rate (~10 s) allowed the probes to quickly solidify upon injection to have a high retention in tissues. The polymeric probes overcame the toxicity issue of current small molecule EPR probes. The probes can be gradually hydrolyzed. Upon complete hydrolysis, the probes became water soluble at 37 °C, thus having the potential to be removed from the body by urinary system. The probes showed slow weight loss rate so as to maintain EPR signal intensity for extended periods while retaining in a certain tissue location. The probes remained their high oxygen sensitivity after in vitro hydrolysis and in vivo implantation for 4 weeks. These hydrogel-based EPR probes have attractive properties for in vivo oxygen detection.

1. Introduction

Oxygen plays an important role in cell metabolism. The decrease of tissue oxygen content due to pathological conditions such as coronary heart disease and stroke, leads to severe cell death and tissue damage [1,2]. Restoration of tissue oxygen content is the primary treatment goal. It may be achieved by vascularization [3,4] or sustained release of oxygen to the tissues [5–7]. To accurately and efficiently assess efficacy of a treatment especially for vascularization therapy that generally takes > 4 weeks, [4,5] long-term (≥ 4 weeks) detection of oxygen concentration in the same tissue location by a minimally invasive or non-invasive spectroscopic approach represents a compelling strategy. However, most existing approaches for oxygen monitoring, such as polarographic electrodes [8], fluorescence-based techniques [9] and pulse oximetry, [10] show unsatisfied performance since they are either invasive or cannot quickly and reproducibly measure oxygen for extended periods.

Electron paramagnetic resonance (EPR), coupled with oxygen sensitive probes, is capable of providing non-invasive, accurate, and rapid measurement of tissue oxygen content [11]. Both water insoluble and soluble oxygen sensitive probes can be used for oxygen detection. Current water insoluble probes are able to measure oxygen concentration for a relatively long time period. Yet they are not degradable or bioeliminable, raising toxicity concerns [12–14]. In contrast, water soluble probes can be readily eliminated from the body [15–18]. Tetrathiatriarylmethyl (TAM) radicals represent a type of soluble probe widely used for tissue oxygen monitoring [11,19–22]. TAM radical have sharp singlet EPR signals, [1,23] and high oxygen sensitivity [24]. However, their relatively low stability when exposed to oxidoreductants in the ischemic tissues, limits their applications. TAM radical

* Corresponding author at: Department of Materials Science and Engineering, The Ohio State University, Columbus, OH 43210, USA.
E-mail address: jguan22@wustl.edu (J. Guan).
[1] These authors contributed equally to this work.

https://doi.org/10.1016/j.msec.2019.02.075
Received 17 December 2018; Received in revised form 6 February 2019; Accepted 20 February 2019
Available online 20 February 2019

quickly lose EPR signals when the radicals are scavenged by oxidoreductants [25,26]. Modification of TAM radical with dendrimers to provide them with shield effect has been shown to improve their stability [26,27]. Conjugation of TAM radical with methoxypoly(ethylene glycol) (mPEG) can also enhance the stability [28]. Short retention time in tissue (typically ≤4 h) is another limitation for TAM radical that does not allow them to be used for long-term oxygen monitoring [29]. Encapsulation of TAM radical within polymers such as poly(vinyl acetate) [22] and Pluronic F-127 [23] can extend the retention time. Yet it is shorter than 5 h [14,30–32]. In addition, the oxygen sensitivity of TAM radical was attenuated due to the poor oxygen permeability of polymers [33]. Modification of TAM radical with dendrimer or mPEG can extend the retention time ≥10 h. However, it is still not long enough for long-term (≥4 weeks) oxygen detection as vascularization process may take several weeks.

The objective of this work was to address the current limitations by creating injectable, bioeliminable, stable, and long retention polymeric TAM probes that can be injected into the diseased tissues for long-term (≥4 weeks) measurement of tissue oxygen concentration during treatment period. These probes also featured fast gelation rate, slow weight loss rate, and high oxygen sensitivity.

2. Materials and methods

2.1. Materials

All chemicals were purchased from Sigma-Aldrich unless otherwise stated. N-Isopropylacrylamide (NIPAAm, VWR) was recrystallized in hexane before use. 2-hydroxyethyl methacrylate (HEMA, Alfa Aesar) and acrylic acid (AAc) was passed through an inhibitor remover column to remove the inhibitors. Dimethyl-γ-butyrolactone acrylate (DBA) was synthesized by acylation of pantolactone [37]. 2,2′-Azobis(2-methylpropionitrile), dioxane, hydrogen peroxide (30% aqueous solution), ascorbic acid (Asc), iron (III) chloride hexahydrate, cesium carbonate (Cs_2CO_3, BTC Beantown Chemical), potasium iodide (KI, BTC Beantown Chemical), nitrilotriacetic acid (NTA, Fisher Scientific), and 1,1,1,3,3,3-hexafluoro-2-propanol (HFIP, Oakwood Chemical) were used as received without further purification. TAM radical was synthesized following a previous report [38]. Bromoethyl methacrylate (BEMA) was synthesized using an established protocol [39].

2.2. Synthesis of hydrogel polymer

The hydrogel was synthesized by free radial polymerization of NIPAAm, HEMA, DBA and BEMA. Molar ratio of the monomers was 60/20/10/10. In brief, NIPAAm, HEMA, DBA and BEMA were dissolved in dioxane in a 3-necked flask with N_2 inlet and outlet. After purging the solution with N_2 for 15 min, AIBN was added into the flask. The reaction was conducted at 70 °C for 6 h (Scheme 1). The solution was then precipitated in hexane. The polymer was purified by dissolving in tetrahydrofuran and precipitating in ethyl ether [40]. Structure of the polymer was determined by ^{1}H NMR spectrum.

2.3. Conjugation of TAM radical onto hydrogel polymer

The hydrogel polymer (0.3 g) and TAM (0.083 g) were dissolved in dimethylformamide. KI (0.014 g) and Cs_2CO_3 (0.095 g) were added into the solution sequentially. After mixing and stirring overnight, the mixture was poured into DI water (Scheme 1). HCl (1 M) was added dropwise to precipitate the polymer (abbreviated as hydrogel-TAM). The hydrogel-TAM was washed with DI water three times and freeze-dried overnight. The structure and composition of the polymer was determined by ^{1}H NMR spectra.

2.4. Characterization of hydrogel-TAM

Hydrogel-TAM solution (10 wt%) was prepared by dissolving the polymer in phosphate buffer saline (PBS, pH = 7.4) at 4 °C. The solution was then transferred into a 37 °C water bath for gelation. Water content of the gel was measured after 24 h of incubation in 37 °C PBS. The weight of the wet (w_1) and the lyophilized gel (w_2) was measured respectively. The water content was calculated as:

$$\text{Water content (\%)} = (w_1 - w_2)/w_2 \times 100\%$$

To test hydrolytic property of hydrogel-TAM, 200 μL hydrogel-TAM solution (10 wt%) was added into each 1.5 mL microtubes. After gelation at 37 °C overnight. The supernatant was replaced with 200 μL PBS. The hydrolysis was conducted at 37 °C for 4 weeks. The samples were taken out at each week, and freeze-dried. The weight before and after hydrolysis was measured as w_3 and w_4, respectively. The weight remaining was calculated as:

$$\text{Weight remaining (\%)} = w_4/w_3 \times 100\%$$

The gelation temperature of the hydrogel-TAM solution was measured using differential scanning calorimetry (DSC). The temperature range and the heating rate were 0–60 °C and 10 °C/min, respectively [5].

Injectability of the hydrogel-TAM solution was evaluated by its ability to go through 22-guage needle. Gelation time was defined as the time needed for the 4 °C hydrogel-TAM solution to become a solid gel at 37 °C, and determined using our previously established protocol [37].

2.5. Oxygen response of hydrogel-TAM

A Bruker EMX plus X-band resonator (9.8 GHz) was used for EPR measurement. Hydrogel-TAM was dissolved in water/DMSO (1/1 by volume) and injected into a gas permeable EPR tube, which was then inserted in the microwave cavity of the EPR resonator. Gas with certain oxygen content was flowed into the tube for at least 15 min to reach the equilibrium. The EPR spectrum was recorded, and EPR linewidth was measured. The linewidths at different oxygen concentrations were obtained using gases with different oxygen contents. At least 3 repeats were used in EPR tests.

2.6. Stability of hydrogel-TAM when exposed to oxidoreductants

To determine stability of the hydrogel-TAM when exposed to oxidoreductants, 3 oxidoreductants were used including H_2O_2 solution (1 mM), ascorbic acid (Asc) solution (1 mM) and hydroxyl radicals (HO·). HO· was prepared following a previously established protocol [28]. In brief, iron (III) chloride solution was slowly added into the NTA solution at the Fe/NTA ratio of 1/2. The mixture was then neutralized to pH 7.4. HO· was generated by adding H_2O_2 solution to the Fe(III)-NTA solution. After mixing each oxidoreductant with hydrogel-TAM for 30 min, EPR signals were monitored. The stability was determined as ratio of the double integral of EPR signals after and before oxidoreductant treatment [28].

2.7. Animal experiments

All animal studies were performed in accordance with the National Institutes of Health Guide for handling laboratory animals. The protocol was approved by Ohio State University Institutional Animal Care and Use Committee. Male 8–10-week-old C57BL/6 mice were used. After anesthesia, 200 μL hydrogel-TAM solution (10 wt%) was injected into thigh muscles by a 22-gauge needle. The tissues were harvested after 3 h and 4 weeks. The hydrogel-TAM was extracted using HFIP. After evaporation of HFIP, the hydrogel-TAM was re-dissolved in water/DMSO (1/1 by volume). EPR linewidths of hydrogel-TAM solution were measured at different oxygen concentrations.

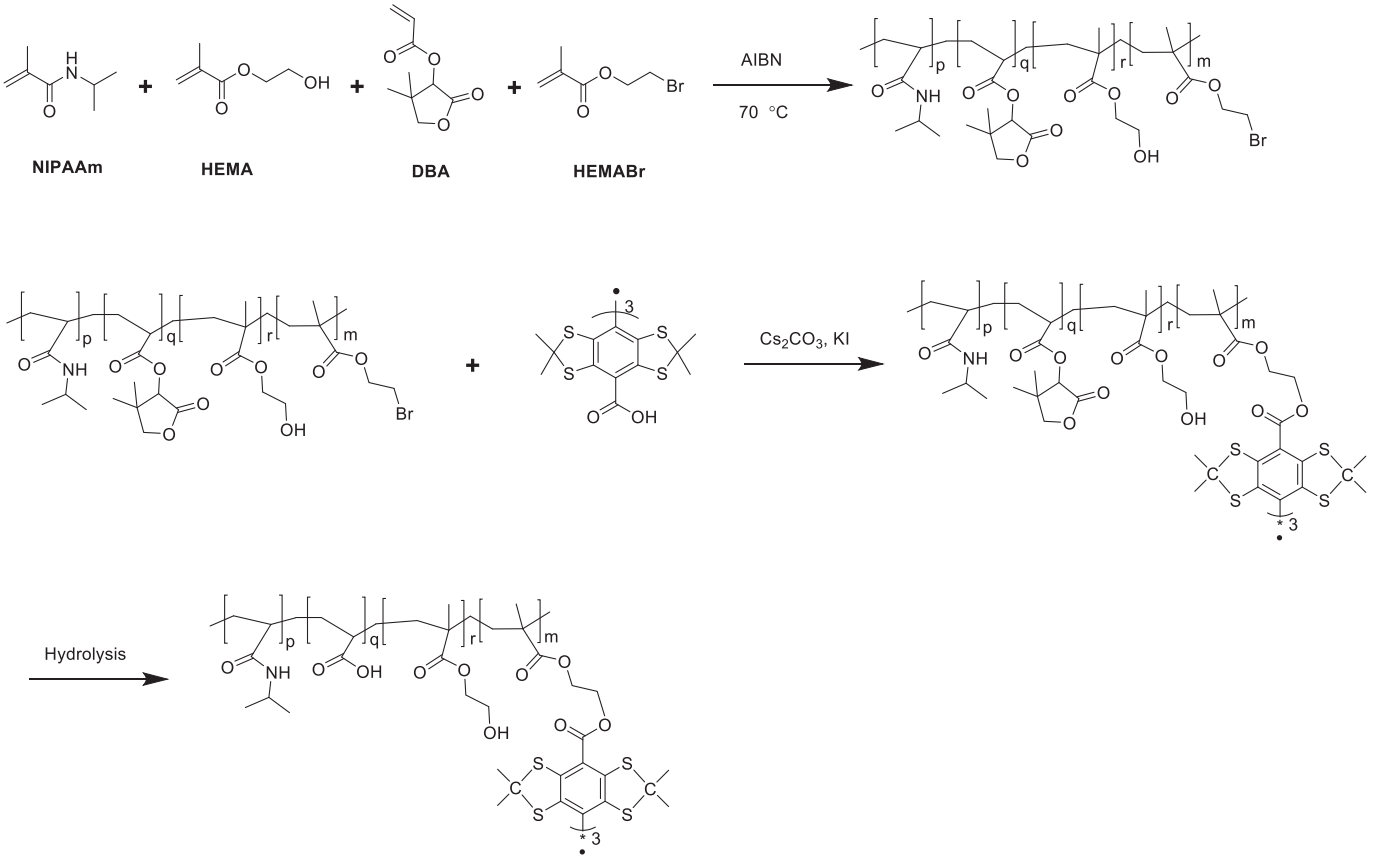

Scheme 1. Synthesis scheme of poly(NIPAAm-co-HEMA-co-DBA-co-BEMA) and hydrogel-TAM.

2.8. Histology and immunohistochemistry

The harvest muscle tissues were fixed by using 4% paraformaldehyde and embedded in paraffin and then sectioned into 4 μm slices. Hematoxylin & Eosin (H&E) staining was performed on the slices and the images were taken using a light microscope. For the immunohistochemistry study, the slices were deparaffinized with xylene and rehydrated with ethanol. After blocking the slices using goat serum, F4/80 primary antibody and Alexa Fluor 488 secondary antibody were used for staining. The images were taken using a confocal microscope. 4 repeats were used to take images in each staining experiments.

2.9. Statistical analysis

Data were presented as mean ± standard deviation. One-way ANOVA was used to analyze the stability of hydrogel-TAM to different oxidoreductants.

3. Results and discussion

3.1. Synthesis of hydrogel-TAM and characterization of properties

The hydrogel polymer was synthesized by free radical polymerization of NIPAAm, HEMA, DBA and BEMA. ^{1}H NMR spectrum (Fig. 1a) confirmed the structure of the polymer. The molar ratio of NIPAAm/HEMA/DBA/BEMA was 60/19/7/14, consistent with the feed ratio. The polymer was then conjugated with TAM radical. After conjugation, TAM radical affected the chemical environment of protons in the hydrogel, leading to the substantial peak shift in the ^{1}H NMR spectrum (Fig. 1b). The appearance of characteristic proton peak for $-C\underline{H}_3$ in the TAM radical in the ^{1}H NMR spectrum of hydrogel-TAM (Fig. 1b) confirmed the successful conjugation. The ratio of conjugation was calculated to be 95%. The successful conjugation is also confirmed by EPR spectra (Fig. 2). At N_2 atmosphere, the hydrogel-TAM showed a narrow singlet peak, same as that of the free TAM radical. The peak-to-peak linewidths of the hydrogel-TAM and TAM radical were 107 ± 1 mG and 105 ± 2 mG, respectively. The neglectable peaks shown in hydrogel-TAM and TAM radical were caused by the hyperfine effect as the unpaired electrons of TAM radical interact with protons located in the methyl group of the TAM radical [41–43]. Protons around TAM radical may affect its stability, leading to the change of linewidth. A previous study demonstrated that conjugation of TAM with mPEG decreased its stability and broadened linewidth [28]. In this work, the conjugation with hydrogel did not compromise TAM stability as the peak-to-peak linewidths of the hydrogel-TAM and TAM radical were similar.

The 4 °C hydrogel solution was flowable and can be readily injected through a 22-gauge needle typically used for muscle injection (Fig. 3). These results demonstrate that the hydrogel solution had appropriate viscosity for delivery into tissues by a minimally invasive injection approach. The hydrogel solution had a sol-gel transition temperature of 33.4 ± 4.9 °C. The 4 °C hydrogel solution formed a solid gel within 10 s when incubated at 37 °C (Fig. 3). The fast gelation rate enables the injected hydrogel-TAM to quickly immobilize in the tissues after injection. The resulting gel exhibited water content of 64.1 ± 4.5%.

The hydrogel-TAM was designed to be bioeliminable after complete hydrolysis of DBA component. The ester group in the DBA component can be slowly hydrolyzed to −COOH group [44]. To determine whether the final hydrolysis product (Scheme 1) is able to dissolve in PBS at 37 °C so that it can be eliminated from body, we synthesized the final hydrolysis product by free radical polymerization of NIPAAm, HEMA, AAc, and BEMA followed by conjugation with TAM radical. Its sol-gel temperature was found to be 57.6 ± 6.1 °C, > 37 °C (Fig. 4a and b). Therefore, the final hydrolysis product will be soluble in body fluid. The

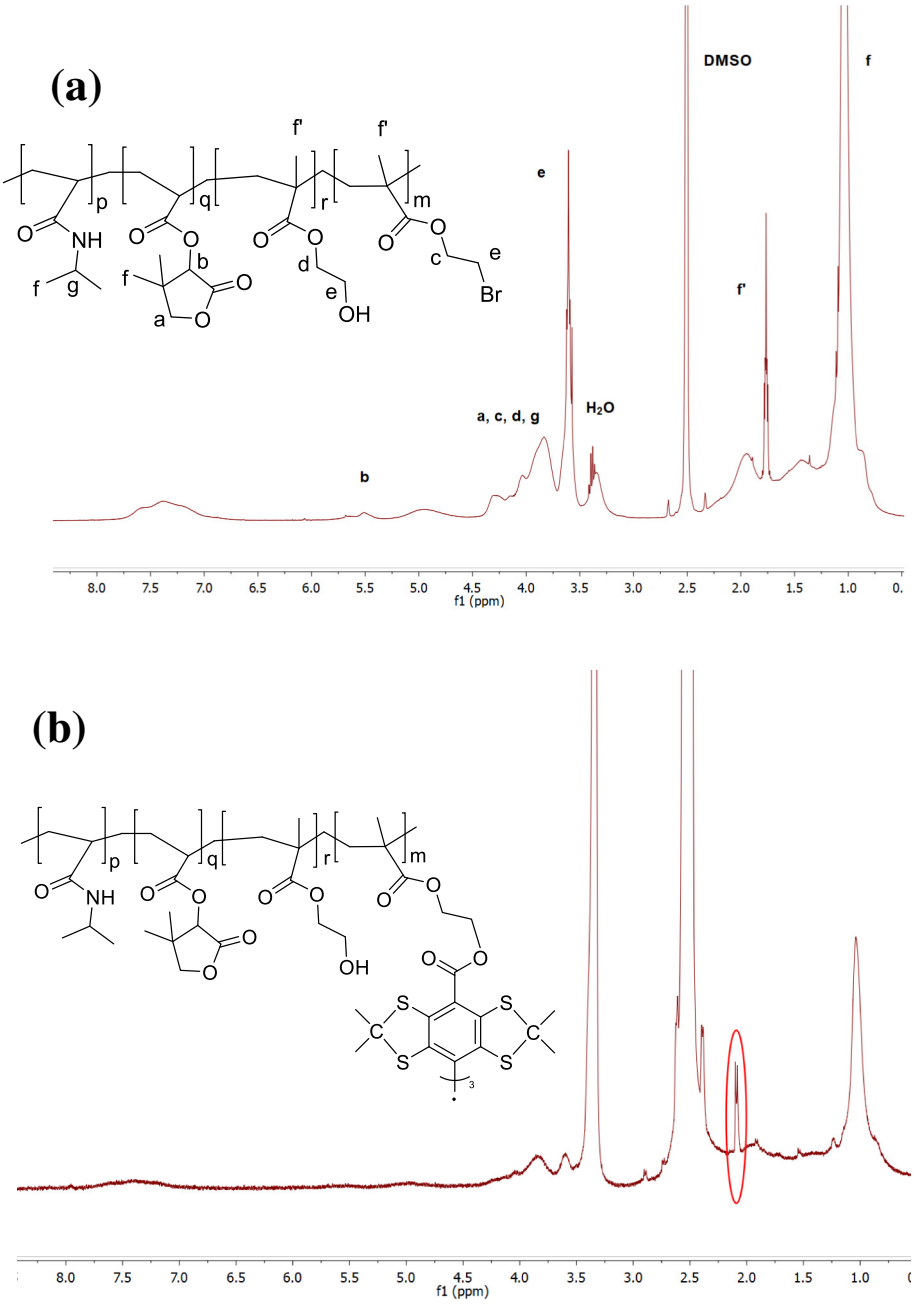

Fig. 1. ^{1}H NMR spectra of poly(NIPAAm-co-HEMA-co-DBA-co-BEMA) (a), and hydrogel-TAM (b). The circled peak in hydrogel-TAM spectrum belongs to TAM radical.

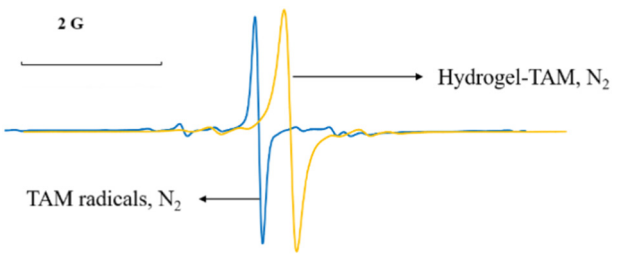

Fig. 2. EPR signals of TAM radical (blue) and hydrogel-TAM (yellow) at N_2 atmosphere. (For interpretation of the references to color in this figure legend, the reader is referred to the web version of this article.)

elevated sol-gel temperature of the final hydrolysis product is likely the result of AAc component increasing hydrophilicity of the polymer [45,46]. To determine hydrolysis rate of the hydrogel-TAM, it was incubated in PBS at 37 °C for 4 weeks. No significant weight loss was observed ($p > 0.05$, weeks 1, 2, 3, and 4 vs. day 0). This is possibly due to slow hydrolysis rate of the DBA component, which has been demonstrated in our previous study [45]. The slow degradation within four weeks met our design goal as it offers the possibility for the hydrogel-TAM to maintain EPR signal intensity for extended periods while retaining in a certain tissue location, allowing for long-term monitoring of oxygen concentration.

3.2. Oxygen response of hydrogel-TAM and sensitivity

To measure oxygen response, gases with different oxygen

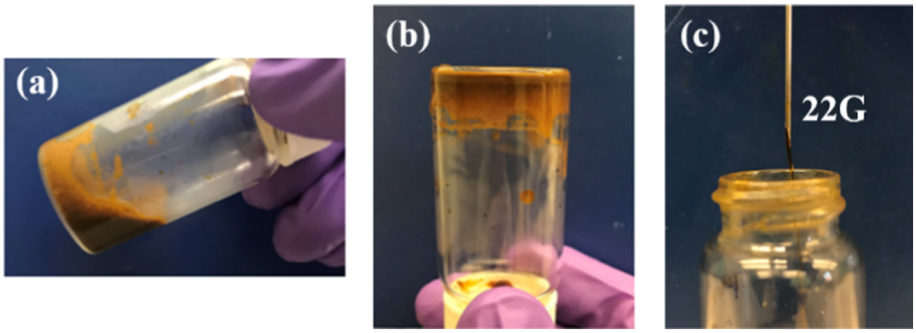

Fig. 3. The synthesized hydrogel-TAM was thermosensitive. It was at liquid state at 4 °C (a) and became a solid gel at 37 °C (b). The hydrogel-TAM was injectable at 4 °C (c).

concentrations (0, 10, 20, 40, 60 and 80%) were flowed through the hydrogel-TAM for at least 15 min, respectively. The peak-to-peak linewidth was then determined from the EPR spectra. The linewidth for the hydrogel-TAM linearly increased from 107 mG to 282 mG when the oxygen concentration was increased from 0% to 80%. A similar linear relationship between the linewidth and oxygen concentration was found for the TAM radical, whose linewidth increased from 105 mG at anaerobic condition to 288 mG at 80% O_2 (Fig. 5). The oxygen sensitivity was calculated as the slope of the linear response of linewidth and oxygen concentration. The hydrogel-TAM possessed the oxygen sensitivity of 0.28 mG/mm Hg, very close to that of the TAM radical (0.30 mG/mm Hg). The similar oxygen sensitivity of hydrogel-TAM and TAM radical further demonstrated that the hydrogel had no substantial influence on the stability of TAM radical.

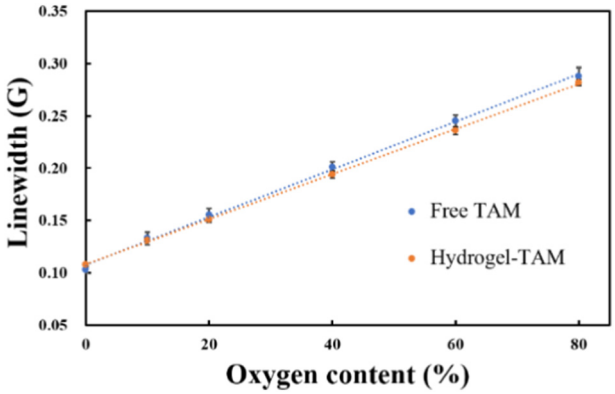

Fig. 5. The linear oxygen-dependent linewidth of hydrogel-TAM and TAM radical measured by EPR.

3.3. Response rate of hydrogel-TAM to oxygen concentration change

Response rate of EPR probe to oxygen concentration change is of importance when using it for real time monitoring of tissue oxygen. Hydrogel-TAM was able to quickly respond to oxygen concentration variation. The response time was within 5 min when the hydrogel-TAM was switched from room air to N_2, and from N_2 to 10% oxygen (Fig. 6a). The hydrogel-TAM exhibited similar response time as the free TAM radical (Fig. 6a).

Linewidth of the hydrogel-TAM was reversible when the oxygen concentration was changed from room air to 0%, and back to room air (Fig. 6b). In addition, the hydrogel-TAM and free TAM radial showed similar linewidth at different oxygen concentrations, and the same duration to reach the equilibrium when switching gases (Fig. 6b). This is possibly because the hydrogel had excellent oxygen permeability. A slightly longer duration for both hydrogel-TAM and free TAM radical to reach the equilibrium was observed when flushing N_2 compared to flowing O_2 (Fig. 6a and b). This is attributed to the lower diffusivity of N_2 [47].

3.4. Oxygen response of hydrogel-TAM during the in vitro hydrolysis

The influence of hydrolysis on the EPR property of hydrogel-TAM was investigated after 1 and 4 weeks of incubation in PBS. The linewidth of remaining hydrogel-TAM showed a linear relationship with oxygen concentration at both time points (Fig. 7). In addition, the linewidth was almost the same at each oxygen concentration after 1 and 4 weeks of hydrolysis. As a result, the oxygen sensitivity was remained similar (0.30 mG/mm Hg for week 1, and 0.28 mG/mm Hg for week 4).

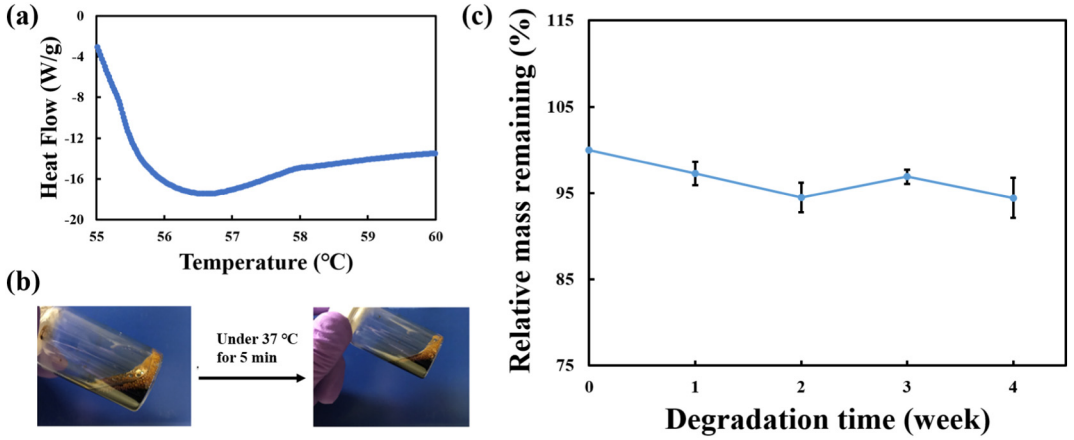

Fig. 4. Sol-gel temperature of the final hydrolysis product of hydrogel-TAM (a). It was soluble at 37 °C after being fully degraded (b). Weight remaining of hydrogel-TAM in PBS for four weeks (c).

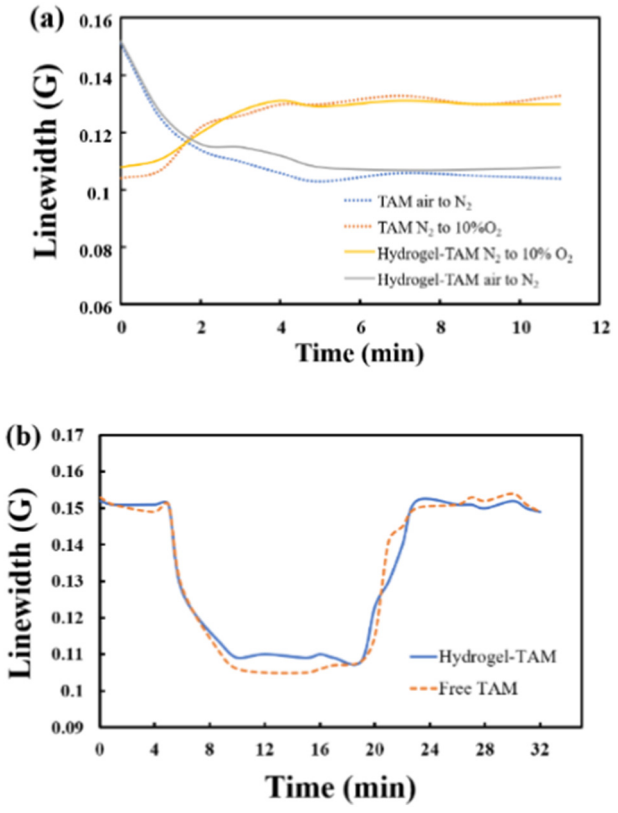

Fig. 6. (a) The influence of oxygenation and deoxygenation on EPR signals of TAM radical and hydrogel-TAM. (b) Reversibility of TAM radical and hydrogel-TAM determined by EPR linewidths changing as a function of time.

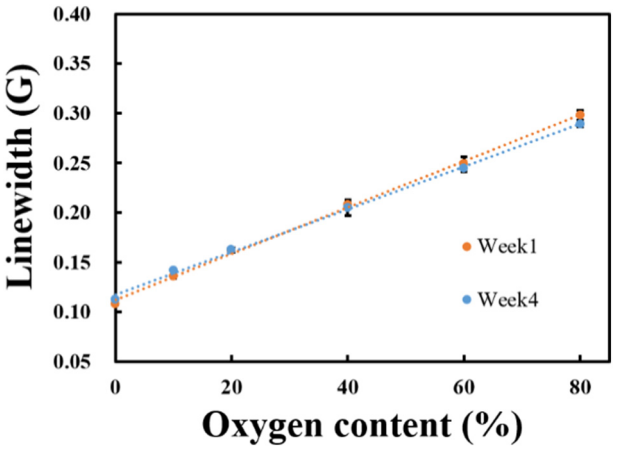

Fig. 7. The influence of hydrogel-TAM degradation in vitro on the linear relationship between the linewidth and oxygen contents.

The oxygen sensitivity was also similar to that of the hydrogel-TAM before degradation. These results demonstrated that the hydrogel-TAM had stable EPR properties during in vitro hydrolysis, possibly due to slow weight loss (Fig. 4C).

3.5. Oxygen response of hydrogel-TAM after in vivo implantation

To investigate the EPR property change of hydrogel-TAM after in vivo implantation, the hydrogel-TAM solution was injected into mouse thigh muscles. The control was free TAM radical. The tissues were harvested at 3 h and 4 weeks of post-implantation, and the hydrogel-TAM was extracted. After only 3 h of implantation, the EPR signals of

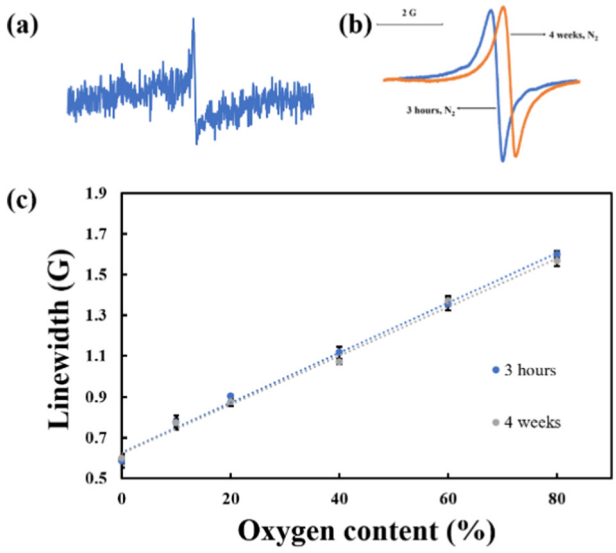

Fig. 8. EPR signals of TAM radical under N_2 following 3 h of implantation (a). EPR signals of hydrogel-TAM in N_2 following 3 h and 4 weeks of implantation (b). The EPR linewidth of hydrogel-TAM as function of the oxygen content after degradation in vivo for four weeks (c). Muscle tissues with hydrogel-TAM were harvested and hydrogel-TAM was extracted by HFIP.

TAM radical under N_2 was largely weakened and strong noise was detected (Fig. 8a). In contrast, sharp and narrow singlet peaks were seen for hydrogel-TAM in N_2 (Fig. 8b). The noise was extremely low. After 4 weeks of implantation, no TAM radical was monitored due to its short retention time in tissue (typically < 4 h). However, the hydrogel-TAM showed similar EPR spectrum as that was implanted for 3 h (Fig. 8b). The peak-to-peak linewidth of hydrogel-TAM showed a linear function with oxygen concentration after 3 h and 4 weeks of implantation (Fig. 8c). In addition, the oxygen sensitivity remained unchanged (1.60 mG/mm Hg at 3 h, and 1.57 mG/mm Hg at 4 weeks). These results demonstrated that the hydrogel-TAM not only extended the retention time of TAM radical in vivo, but also had stable oxygen responsiveness and sensitivity. The retention time of the hydrogel-TAM was also remarkably longer than those chemically modified TAM radical whose half-life was only several hours [28,38]. Encapsulation of TAM radical into polydimethylsiloxane (PDMS) can prolong its retention time in vivo [48]. However, PDMS is non-degradable and non-injectable. It needs invasive surgeries to implant and retrieve, thus having lower clinical significance. The hydrogel-TAM in this work is not only injectable, but also bioeliminable. Therefore, minimally invasive injection approach can be used for implantation, and retrieval is not necessary. Although we designed the hydrogel-TAM to have no significant weight loss in the 4-week study period, the ester group in the DBA component can be slowly hydrolyzed (Scheme 1) resulting in the final hydrolysis product that is soluble in body fluid. The long retention time and stable oxygen sensitivity allow the hydrogel-TAM to be used for long-term monitoring of tissue oxygen. It should be noted that the linewidth of hydrogel-TAM after implantation was broadened. Same phenomena was found for the free TAM radical [28]. This is likely resulted from the binding of TAM radical with plasma proteins in tissues [28]. One of the potential challenges in using hydrogel-TAM for long-term monitoring of tissue oxygen is that more plasma proteins may bind to the TAM radical as vascularization progresses. This may further broaden EPR linewidth and affect oxygen sensitivity. Use of hydrogels with lower water content may address the challenge as it will decrease plasma protein penetration to the hydrogel, thus reducing binding to TAM radical.

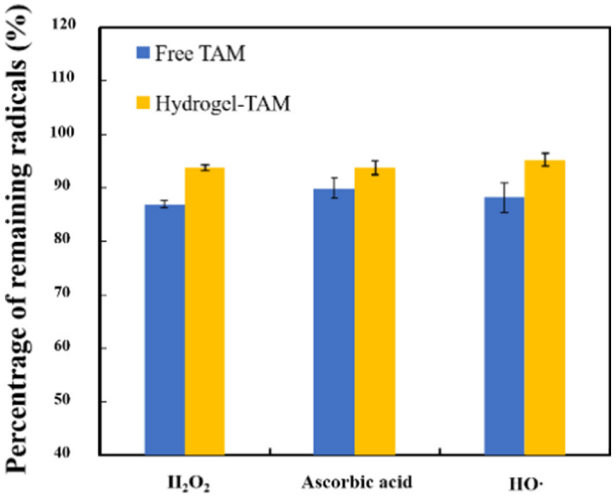

Fig. 9. The stability of hydrogel-TAM towards oxidoreductants after being exposed for 30 min. The concentration of oxidoreductants was maintained at 1 mM.

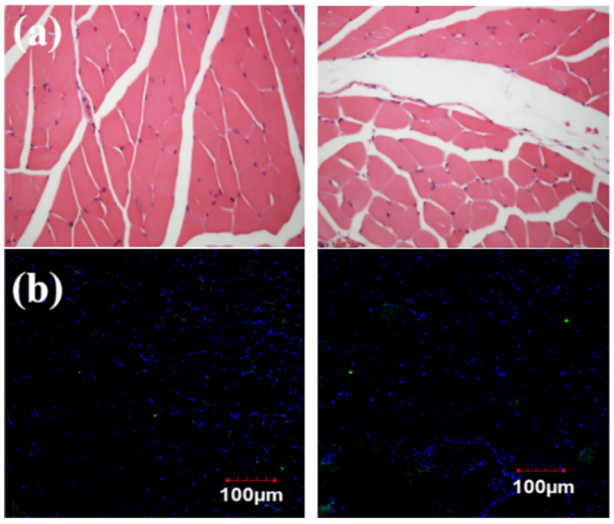

Fig. 10. H&E (a) and F4/80 (b) stainings of muscle tissues without (left column) and with (right column) injection of hydrogel-TAM.

3.6. Stability of hydrogel-TAM when exposed to oxidoreductants

Ischemic tissues typically contain oxidoreductants that compromise the stability of TAM radical. For example, reducing agent Asc leads to reduction of TAM radical, and oxidizing agents such as H_2O_2 and HO· induce the oxidization of TAM radical, resulting in a spin-loss reaction of TAM radical [26,49,50]. To determine whether conjugation with hydrogel can improve its stability, the hydrogel-TAM was exposed to Asc, H_2O_2 and HO·. After 30 min, the remaining TAM radical in the hydrogel-TAM was only quenched < 7% regardless of the type of oxidoreductant (Fig. 9). However, the remaining free TAM radical was only 87% in H_2O_2, 90% in Asc and 88% in HO·, respectively, consistent with the previous study [26]. These results demonstrate that the conjugation with hydrogel significantly increased TAM radical stability in the presence of oxidoreductants ($p < 0.05$ for hydrogel-TAM vs. TAM in all 3 oxidoreductants). It is possible that the long polymer chains in the hydrogel acted as a barrier to prevent oxidoreductants from attacking conjugated TAM radicals. Similar results were reported previously where the conjugation of TAM radical with dendritic poly (ethylene glycol) greatly improved the its stability towards oxidoreductants [26].

3.7. In vivo biocompatibility of hydrogel-TAM

After implantation for 4 weeks, the thigh muscles were harvested, and H&E (Fig. 10a) and F4/80 (Fig. 10b) stainings were performed. The implanted hydrogel was not fully degraded and the remaining hydrogel (large white gap between muscles) can be seen in Fig. 10a. H&E staining demonstrated that hydrogel-TAM implantation did not substantially increase tissue inflammation compared to the normal muscle tissue. In F4/80 staining, only few macrophages were seen in the hydrogel-TAM implanted muscle, and normal muscle. TAM radical is usually used at a low concentration (below 1 mM) due to toxicity concern [34–36]. The H&E and F4/80 staining results demonstrate that the TAM radical in the hydrogel-TAM did not cause tissue death and inflammation. Therefore, the hydrogel-TAM had excellent biocompatibility.

The stable oxygen sensitivity, fast gelation rate, high stability towards oxidoreductants, and excellent biocompatibility make the developed probes promising for oxygen monitoring in tissues. In our future studies, we will implant the probes for real time and long-term (≥4 weeks) detecting tissue oxygen concentration during vascularization therapy.

4. Conclusion

Polymer-based TAM radical (Hydrogel-TAM) was synthesized by conjugating TAM radical to a thermosensitive, fast gelation, and bioeliminable hydrogel. The hydrogel-TAM showed linear response of linewidth and oxygen concentration. It also preserved high oxygen sensitivity and response rate to oxygen concentration change of the free TAM radical. The hydrogel-TAM was stable during the 4-week in vitro and in vivo degradation with oxygen sensitivity unchanged. Furthermore, the hydrogel-TAM possessed a higher stability to oxidoreductants than free TAM radical. To the best of our knowledge, hydrogel-TAM is the first bioeliminable, polymeric EPR probe that can be minimally invasively injected into tissue and had a prolonged retention time in tissue.

Acknowledgements

We appreciate the assistance from Dr. Gordan Renkes.

Funding sources

This work was supported by US National Institutes of Health (R01HL138175, R01HL138353, R01EB022018, R01AG056919 and R21EB021896) and National Science Foundation (1708956).

References

[1] J.H. Ardenkjær-Larsen, I. Laursen, I. Leunbach, G. Ehnholm, L.-G. Wistrand, J.S. Petersson, K. Golman, EPR and DNP properties of certain novel single electron contrast agents intended for oximetric imaging, J. Magn. Reson. 133 (1998) 1–12, https://doi.org/10.1006/jmre.1998.1438.
[2] J. Guan, F. Wang, Z. Li, J. Chen, X. Guo, J. Liao, N.I. Moldovan, The stimulation of the cardiac differentiation of mesenchymal stem cells in tissue constructs that mimic myocardium structure and biomechanics, Biomaterials. 32 (2011) 5568–5580, https://doi.org/10.1016/j.biomaterials.2011.04.038.
[3] H.G. Kopp, C.A. Ramos, S. Rafii, Contribution of endothelial progenitors and proangiogenic hematopoietic cells to vascularization of tumor and ischemic tissue, Curr. Opin. Hematol. 13 (2006) 175–181, https://doi.org/10.1097/01.moh.0000219664.26528.da.
[4] C. Rinsch, P. Quinodoz, B. Pittet, N. Alizadeh, D. Baetens, D. Montandon, P. Aebischer, M.S. Pepper, Delivery of FGF-2 but not VEGF by encapsulated genetically engineered myoblasts improves survival and vascularization in a model of acute skin flap ischemia, Gene Ther. 8 (2001) 523–533, https://doi.org/10.1038/sj.gt.3301436.
[5] Z. Li, X. Guo, J. Guan, An oxygen release system to augment cardiac progenitor cell survival and differentiation under hypoxic condition, Biomaterials. 33 (2012) 5914–5923, https://doi.org/10.1016/j.biomaterials.2012.05.012.
[6] T. Komatsu, Y. Oguro, A. Nakagawa, E. Tsuchida, Albumin clusters: structurally defined protein tetramer and oxygen carrier including thirty-two iron(II)

porphyrins, Biomacromolecules. 6 (2005) 3397–3403, https://doi.org/10.1021/bm050454u.
[7] R.M. Wang, T. Komatsu, A. Nakagawa, E. Tsuchida, Human serum albumin bearing covalently attached iron(II) porphyrins as O_2-coordination sites, Bioconjug. Chem. 16 (2005) 23–26, https://doi.org/10.1021/bc049859m.
[8] L.C. Clark Jr., G. Misrahy, R.P. Fox, Chronically implanted polarographic electrodes, J. Chem. Inf. Model. (1958) 1689–1699, https://doi.org/10.1017/CBO9781107415324.004.
[9] J.R. Griffiths, S.P. Robinson, The OxyLite: a fibre-optic oxygen sensor, Br. J. Radiol. 72 (1999) 627–630, https://doi.org/10.1259/bjr.72.859.10624317.
[10] J.T. Moller, T. Pedersen, L.S. Rasmussen, P.F. Jensen, B.D. Pedersen, O. Ravlo, N.H. Rasmussen, K. Espersen, N.W. Johannessen, J.B. Cooper, J.S. Gravenstein, B. Chraemmer-Jorgensen, F. Wiberg-Jorgensen, M. Djernes, L. Heslet, S.H. Johansen, Randomized evaluation of pulse oximetry in 20,802 patients: I. Design, demography, pulse oximetry failure rate, and overall complication rate, Anesthesiology. 78 (1993) 436–444, https://doi.org/10.1097/00000542-199303000-00006.
[11] V.K. Kutala, N.L. Parinandi, R.P. Pandian, P. Kuppusamy, Simultaneous measurement of oxygenation in intracellular and extracellular compartments of lung microvascular endothelial cells, Antioxid. Redox Signal. 6 (2004) 597–603, https://doi.org/10.1089/152308604773934350.
[12] H.M. Swartz, R.B. Clarkson, The measurement of oxygen in vivo using EPR techniques, Phys. Med. Biol. 43 (1998) 1957–1975, https://doi.org/10.1088/0031-9155/43/7/017.
[13] H.M. Swartz, Using EPR to measure a critical but often unmeasured component of oxidative damage: oxygen, Antioxid. Redox Signal. 6 (2004) 677–686, https://doi.org/10.1089/152308604773934440.
[14] V.P. Bhallamudi, R. Xue, C.M. Purser, K.F. Presley, Y.K. Banasavadi-Siddegowda, J. Hwang, B. Kaur, P.C. Hammel, M.G. Poirier, J.J. Lannutti, R.P. Pandian, Nanofiber-based paramagnetic probes for rapid, real-time biomedical oximetry, Biomed. Microdevices 18 (2016), https://doi.org/10.1007/s10544-016-0063-1.
[15] B. Gallez, C. Baudelet, B.F. Jordan, Assessment of tumor oxygenation by electron paramagnetic resonance: principles and applications, NMR Biomed. 17 (2004) 240–262, https://doi.org/10.1002/nbm.900.
[16] M.C. Krishna, S. English, K. Yamada, J. Yoo, R. Murugesan, N. Devasahayam, J.A. Cook, K. Golman, J.H. Ardenkjaer-Larsen, S. Subramanian, J.B. Mitchell, Overhauser enhanced magnetic resonance imaging for tumor oximetry: coregistration of tumor anatomy and tissue oxygen concentration, Proc. Natl. Acad. Sci. 99 (2002) 2216–2221, https://doi.org/10.1073/pnas.042671399.
[17] K.H. Ahn, G. Scott, P. Stang, S. Conolly, D. Hristov, Multiparametric imaging of tumor oxygenation, redox status, and anatomical structure using overhauser-enhanced MRI-prepolarized MRI system, Magn. Reson. Med. 65 (2011) 1416–1422, https://doi.org/10.1002/mrm.22732.
[18] F. Hyodo, R. Murugesan, K. ichiro Matsumoto, E. Hyodo, S. Subramanian, J.B. Mitchell, M.C. Krishna, Monitoring redox-sensitive paramagnetic contrast agent by EPRI, OMRI and MRI, J. Magn. Reson. 190 (2008) 105–112, https://doi.org/10.1016/j.jmr.2007.10.013.
[19] M. Elas, B.B. Williams, A. Parasca, C. Mailer, C.A. Pelizzari, M.A. Lewis, J.N. River, G.S. Karczmar, E.D. Barth, H.J. Halpern, Quantitative tumor oxymetric images from 4D electron paramagnetic resonance imaging (EPRI): methodology and comparison with blood oxygen level-dependent (BOLD) MRI, Magn. Reson. Med. 49 (2003) 682–691, https://doi.org/10.1002/mrm.10408.
[20] K.-I. Yamada, R. Murugesan, N. Devasahayam, J.A. Cook, J.B. Mitchell, S. Subramanian, M.C. Krishna, Evaluation and comparison of pulsed and continuous wave radiofrequency electron paramagnetic resonance techniques for in vivo detection and imaging of free radicals, J. Magn. Reson. 154 (2002) 287–297, https://doi.org/10.1006/jmre.2001.2487.
[21] Y. Liu, F.A. Villamena, J. Sun, Y. Xu, I. Dhimitruka, J.L. Zweier, Synthesis and characterization of ester-derivatized tetrathiatriarylmethyl radicals as intracellular oxygen probes, J. Org. Chem. 73 (2008) 1490–1497, https://doi.org/10.1021/jo7022747.
[22] Y. Liu, F.A. Villamena, J. Sun, T. yao Wang, J.L. Zweier, Esterified trityl radicals as intracellular oxygen probes, Free Radic. Biol. Med. 46 (2009) 876–883, https://doi.org/10.1016/j.freeradbiomed.2008.12.011.
[23] T.J. Reddy, T. Iwama, H.J. Halpern, V.H. Rawal, General synthesis of persistent trityl radicals for EPR imaging of biological systems, J. Org. Chem. 67 (2002) 4635–4639, https://doi.org/10.1021/jo011068f.
[24] I. Dhimitruka, A.A. Bobko, T.D. Eubank, D.A. Komarov, V.V. Khramtsov, Phosphonated trityl probes for concurrent in vivo tissue oxygen and pH monitoring using electron paramagnetic resonance-based techniques, J. Am. Chem. Soc. 135 (2013) 5904–5910, https://doi.org/10.1021/ja401572r.
[25] C. Rizzi, A. Samouilov, V. Kumar Kutala, N.L. Parinandi, J.L. Zweier, P. Kuppusamy, Application of a trityl-based radical probe for measuring superoxide, Free Radic. Biol. Med. 35 (2003) 1608–1618, https://doi.org/10.1016/j.freeradbiomed.2003.09.014.
[26] Y. Song, Y. Liu, C. Hemann, F.A. Villamena, J.L. Zweier, Esterified dendritic TAM radicals with very high stability and enhanced oxygen sensitivity, J. Org. Chem. 78 (2013) 1371–1376, https://doi.org/10.1021/jo301849k.
[27] Y. Liu, F.A. Villamena, J.L. Zweier, Highly stable dendritic trityl radicals as oxygen and pH probe, Chem. Commun. (2008) 4336, https://doi.org/10.1039/b807406b.
[28] W. Liu, J. Nie, X. Tan, H. Liu, N. Yu, G. Han, Y. Zhu, F.A. Villamena, Y. Song, J.L. Zweier, Y. Liu, Synthesis and characterization of PEGylated trityl radicals: effect of PEGylation on physicochemical properties, J. Org. Chem. 82 (2017) 588–596, https://doi.org/10.1021/acs.joc.6b02590.
[29] H. Li, Y. Deng, G. He, P. Kuppusamy, D.J. Lurie, J.L. Zweier, Proton electron double resonance imaging of the in vivo distribution and clearance of a triaryl methyl radical in mice, Magn. Reson. Med. 48 (2002) 530–534, https://doi.org/10.1002/mrm.10222.
[30] J. Frank, M. Elewa, M.M. Said, H.A. El Shihawy, M. El-Sadek, D. Müller, A. Meister, G. Hause, S. Drescher, H. Metz, P. Imming, K. Mäder, Synthesis, characterization, and nanoencapsulation of tetrathiatriarylmethyl and tetrachlorotriarylmethyl (trityl) radical derivatives??-a study to advance their applicability as in vivo EPR oxygen sensors, J. Org. Chem. 80 (2015) 6754–6766, https://doi.org/10.1021/acs.joc.5b00918.
[31] R.P. Pandian, G. Meenakshisundaram, A. Bratasz, E. Eteshola, S.C. Lee, P. Kuppusamy, An implantable Teflon chip holding lithium naphthalocyanine microcrystals for secure, safe, and repeated measurements of pO_2 in tissues, Biomed. Microdevices 12 (2010) 381–387, https://doi.org/10.1007/s10544-009-9394-5.
[32] G. Meenakshisundaram, R.P. Pandian, E. Eteshola, S.C. Lee, P. Kuppusamy, A paramagnetic implant containing lithium naphthalocyanine microcrystals for high-resolution biological oximetry, J. Magn. Reson. 203 (2010) 185–189, https://doi.org/10.1016/j.jmr.2009.11.016.
[33] I.M.A. Diniz, C. Chen, X. Xu, S. Ansari, H.H. Zadeh, M.M. Marques, S. Shi, A. Moshaverinia, Pluronic F-127 hydrogel as a promising scaffold for encapsulation of dental-derived mesenchymal stem cells, J. Mater. Sci. Mater. Med. 26 (2015) 1–10, https://doi.org/10.1007/s10856-015-5493-4.
[34] Y. Liu, F.A. Villamena, Y. Song, J. Sun, A. Rockenbauer, J.L. Zweier, Synthesis of 14N- and 15N-labeled trityl-nitroxide biradicals with strong spin-spin interaction and improved sensitivity to redox status and oxygen, J. Org. Chem. 75 (2010) 7796–7802, https://doi.org/10.1021/jo1016844.
[35] N. Khan, J.P. Blinco, S.E. Bottle, K. Hosokawa, H.M. Swartz, A.S. Micallef, The evaluation of new and isotopically labeled isoindoline nitroxides and an azaphenalene nitroxide for EPR oximetry, J. Magn. Reson. (2011), https://doi.org/10.1016/j.jmr.2011.05.007.
[36] L. Lampp, O.Y. Rogozhnikova, D.V. Trukhin, V.M. Tormyshev, M.K. Bowman, N. Devasahayam, M.C. Krishna, K. Mäder, P. Imming, A radical containing injectable in-situ-oleogel and emulgel for prolonged in-vivo oxygen measurements with CW EPR, Free Radic. Biol. Med. (2019), https://doi.org/10.1016/j.freeradbiomed.2018.10.442.
[37] Z. Li, F. Wang, S. Roy, C.K. Sen, J. Guan, Injectable, highly flexible, and thermosensitive hydrogels capable of delivering superoxide dismutase, Biomacromolecules. 10 (2009) 3306–3316, https://doi.org/10.1021/bm900900e.
[38] I. Dhimitruka, M. Velayutham, A.A. Bobko, V.V. Khramtsov, F.A. Villamena, C.M. Hadad, J.L. Zweier, Large-scale synthesis of a persistent trityl radical for use in biomedical EPR applications and imaging, Bioorganic Med. Chem. Lett. 17 (2007) 6801–6805, https://doi.org/10.1016/j.bmcl.2007.10.030.
[39] Z. Wang, N.V. Tsarevsky, Well-defined polymers containing high density of pendant viologen groups, J. Polym. Sci. Part A Polym. Chem. 55 (2017) 1173–1182, https://doi.org/10.1002/pola.28474.
[40] Z. Li, X. Guo, A.F. Palmer, H. Das, J. Guan, High-efficiency matrix modulus-induced cardiac differentiation of human mesenchymal stem cells inside a thermosensitive hydrogel, Acta Biomater. 8 (2012) 3586–3595, https://doi.org/10.1016/j.actbio.2012.06.024.
[41] N.J. Bunce, Introduction to the interpretation of electron spin resonance spectra of organic radicals, J. Chem. Educ. 64 (1987) 907, https://doi.org/10.1021/ed064p907.
[42] D.J. Griffiths, Hyperfine splitting in the ground state of hydrogen, Am. J. Phys. 50 (1982) 698–703, https://doi.org/10.1119/1.12733.
[43] B. Driesschaert, V. Marchand, P. Levêque, B. Gallez, J. Marchand-Brynaert, A phosphonated triarylmethyl radical as a probe for measurement of pH by EPR, Chem. Commun. 48 (2012) 4049, https://doi.org/10.1039/c2cc00025c.
[44] Z. Cui, B.H. Lee, C. Pauken, B.L. Vernon, Degradation, cytotoxicity, and biocompatibility of NIPAAm-based thermosensitive, injectable, and bioresorbable polymer hydrogels, J. Biomed. Mater. Res. A (2011), https://doi.org/10.1002/jbm.a.33093.
[45] Z. Li, X. Guo, S. Matsushita, J. Guan, Differentiation of cardiosphere-derived cells into a mature cardiac lineage using biodegradable poly(N-isopropylacrylamide) hydrogels, Biomaterials. 32 (2011) 3220–3232, https://doi.org/10.1016/j.biomaterials.2011.01.050.
[46] J. Guan, Y. Hong, Z. Ma, W.R. Wagner, Protein-reactive, thermoresponsive copolymers with high flexibility and biodegradability, Biomacromolecules. 9 (2008) 1283–1292, https://doi.org/10.1021/bm701265j.
[47] R.P. Pandian, Y.-I. Kim, P.M. Woodward, J.L. Zweier, P.T. Manoharan, P. Kuppusamy, The open molecular framework of paramagnetic lithium octabutoxy-naphthalocyanine: implications for the detection of oxygen and nitric oxide using EPR spectroscopy, J. Mater. Chem. 16 (2006) 3609–3618, https://doi.org/10.1039/b517976a.
[48] H. Hou, N. Khan, M. Nagane, S. Gohain, E.Y. Chen, L.A. Jarvis, P.E. Schaner, B.B. Williams, A.B. Flood, H.M. Swartz, P. Kuppusamy, Skeletal muscle oxygenation measured by EPR oximetry using a highly sensitive polymer-encapsulated paramagnetic sensor, Adv. Exp. Med. Biol, 2016, pp. 351–357, , https://doi.org/10.1007/978-3-319-38810-6_46.
[49] Y. Liu, Y. Song, F. De Pascali, X. Liu, F.A. Villamena, J.L. Zweier, Tetrathiatriarylmethyl radical with a single aromatic hydrogen as a highly sensitive and specific superoxide probe, Free Radic. Biol. Med. 53 (2012) 2081–2091, https://doi.org/10.1016/j.freeradbiomed.2012.09.011.
[50] C. Decroos, Y. Li, A. Soltani, Y. Frapart, D. Mansuy, J.L. Boucher, Oxidative decarboxylation of tris-(p-carboxyltetrathiaaryl)methyl radical EPR probes by peroxidases and related hemeproteins: intermediate formation and characterization of the corresponding cations, Arch. Biochem. Biophys. 502 (2010) 74–80, https://doi.org/10.1016/j.abb.2010.07.002.